



# *Self-consistency, collective excitations and full resummation of many-body Green's functions*

**Carlo Barbieri**

- Optimizing reference states
- Polarization propagators from SCGF - Two-phonon version
- Diagrammatic Monte Carlo for the Richardson pairing
- Gorkov-SCGF in nuclear matter (there's no time)

# (Ab Initio) Optical potentials workshop at the ECT\*

## TOWARDS A CONSISTENT APPROACH FOR NUCLEAR STRUCTURE AND REACTIONS: MICROSCOPIC OPTICAL POTENTIALS

**June 17-24, 2024**



17 June 2024 — 21 June 2024

### Organizers

**Carlo Barbieri (Università degli Studi di Milano)**

[carlo.barbieri@unimi.it](mailto:carlo.barbieri@unimi.it)

**Charlotte Elster (Ohio University)**

[elster@ohio.edu](mailto:elster@ohio.edu)

**Chloë Hebborn (Facility of Rare Isotopes Beams (FRIB))**

[hebborn@frib.msu.edu](mailto:hebborn@frib.msu.edu)

**Alexandre Obertelli (TU Darmstadt)**

[aobertelli@ikp.tu-darmstadt.de](mailto:aobertelli@ikp.tu-darmstadt.de)

Direct nuclear reactions, processes such as nucleon transfer, knockout, anti-nucleon capture have been extensively exploited by experiments to learn about the structure of exotic isotopes far away from stability, to infer properties of the nuclear forces, to describe nucleosynthesis and to learn about the nuclear equation of state. In this respect, nucleon-nucleus optical potentials are of great importance since they are the fundamental building blocks needed to predict reaction observables to address such a wide range of Nuclear Physics facets. Traditional phenomenological optical potential parameterizations are fully reliable only in specific regions of the nuclear chart, near the stable isotopes they were fitted to. On the contrary, microscopically derived potentials can be systematically extended to isotopes far from stability that are the focus of modern experimental searches. This workshop will address the state-of-the-art of nuclear optical potentials to foster advances in their accuracy and handling of uncertainty propagation.



UNIVERSITÀ DEGLI STUDI DI MILANO

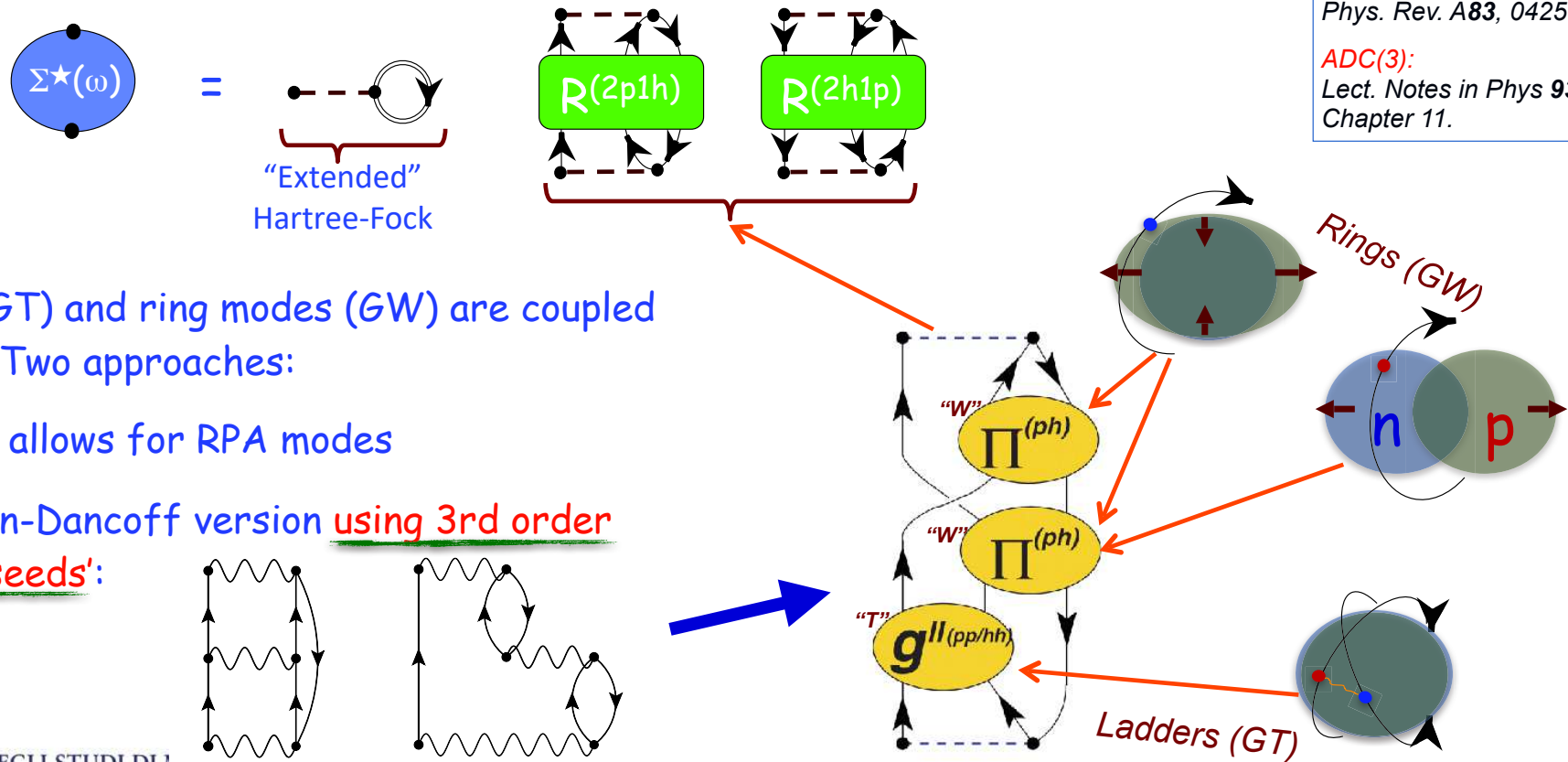
DIPARTIMENTO DI FISICA



# The Faddeev-RPA and ADC(3) methods in a few words

Compute the nuclear self energy to extract both scattering (optical potential) and spectroscopy.

Both ladders and rings are needed for atomi nuclei:

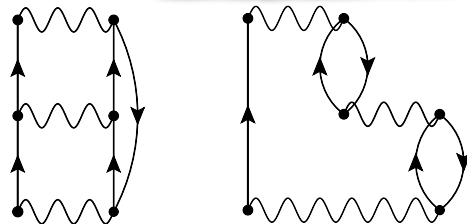


**F-RPA:**  
 Phys. Rev. C **63**, 034313 (2001)  
 Phys. Rev. A **76**, 052503 (2007)  
 Phys. Rev. A **83**, 042517 (2011)

**ADC(3):**  
 Lect. Notes in Phys **936** (2017)-  
 Chapter 11.

All Ladders (GT) and ring modes (GW) are coupled to all orders. Two approaches:

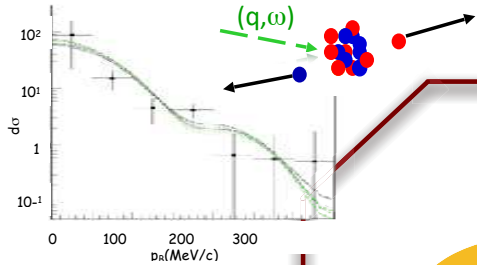
- Faddeev-RPA allows for RPA modes
- ADC(3) Tamn-Dancoff version using 3rd order diagrams as 'seeds':



# The Self-Consistent Green's Function with Faddeev-RPA

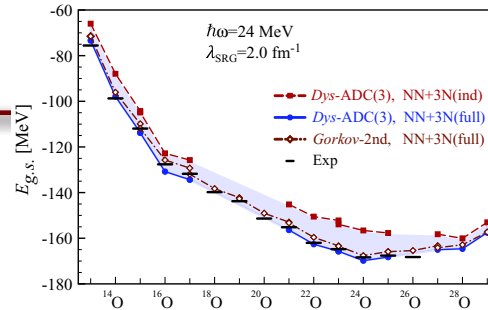
## Two-nucleon emission: $^{16}\text{O}(e,e'pn)^{14}\text{N}$

[Eur. Phys. J. A43, 137 (2010)]



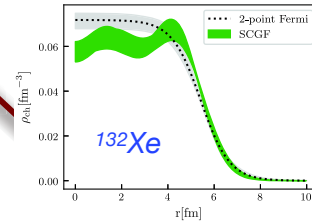
## Binding energies

Oxygen drip line  
[Phys. Rev. Lett. 111, 062501 (2013)]



## Charge & matter distribution

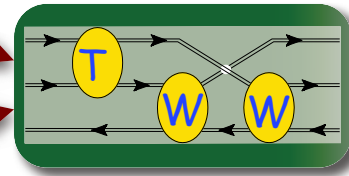
Neutron skins [Phys. Rev. Lett. 125, 182501 (2020)]



	SCGF	Exp.
$^{100}\text{Sn}$	4.525 – 4.707	
$^{132}\text{Sn}$	4.725 – 4.956	4.7093
$^{132}\text{Xe}$	4.700 – 4.948	4.7859
$^{136}\text{Xe}$	4.715 – 4.928	4.7964
$^{138}\text{Xe}$	4.724 – 4.941	4.8279

T ladders

W rings



Dyson Eq.

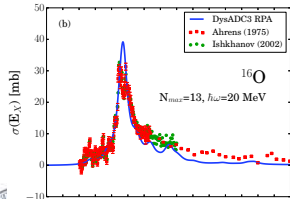
## Spectroscopy

Ionisation energies and affinities for simple atoms and molecules  
[Phys. Rev. A. 83, 042517 (2011); 85, 012501 (2012)]

	Level	ADC(3)	FRPA	FRPA(c)	Expt.
HF	1π	16.48	16.05	16.35	16.05
	3σ	20.36	20.03	20.24	20.0
CO	5σ	13.94	14.37	13.69	14.01
	1π	16.98	16.95	16.84	16.91
	4σ	20.19	19.46	19.59	19.72
H <sub>2</sub> O	1b <sub>1</sub>	12.86	12.62	12.67	12.62
	3a <sub>1</sub>	15.15	14.91	14.98	14.74
	1b <sub>2</sub>	19.21	19.06	19.13	18.51
	$\bar{\Delta}$ (eV)	0.30(0.30)	0.25(0.23)	0.31(0.26)	
	$\Delta_{\text{max}}$ (eV)	0.70(0.70)	0.73(0.73)	0.88(0.62)	

## Nuclear ELM response and dipole polarisability, $\alpha_D$

[Phys. Rev. C99, 054327 (2019)]

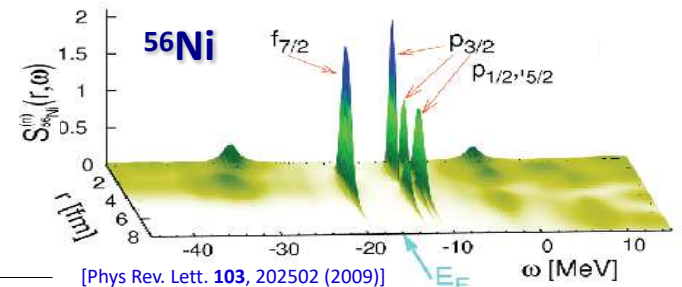
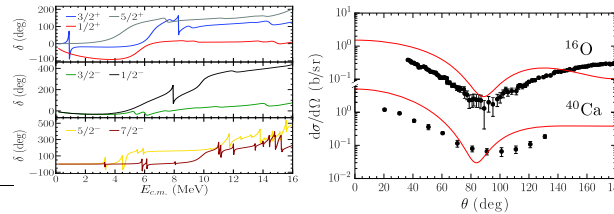


$^{68}\text{Ni}$ :

	SCGF	Exp.
$E_{\text{DIP}}$ (MeV)	10.68	9.55(17)
	10.92	
$E_{\text{CDR}}$ (MeV)	18.1	17.1(2)
$\alpha_D$ (fm <sup>3</sup> )	3.60	3.40(23)
		3.88(31)

## Optical potential

Elastic neutron scattering [Phys. Rev. Lett. 123, 092501 (2013)]

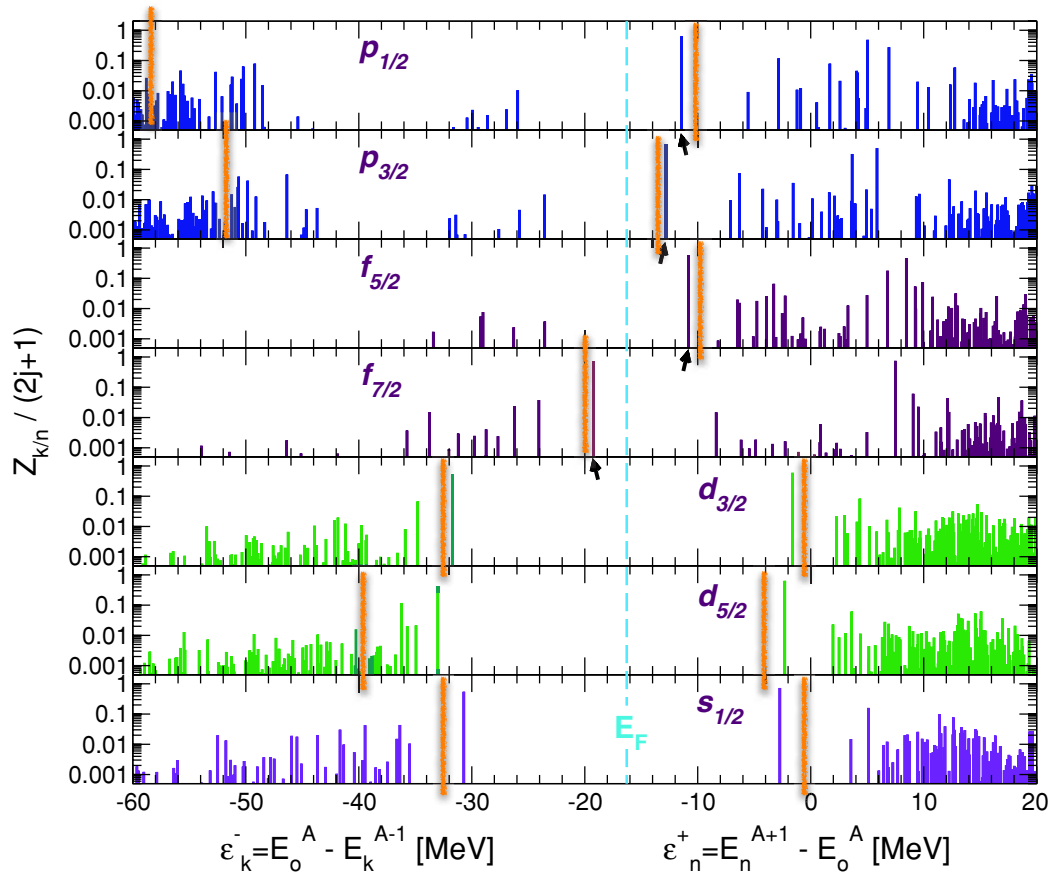


[Phys. Rev. Lett. 103, 202502 (2009)]





## Ni56 one-body propagator decomposed in its partial waves (FRPA, Max=9):



$$g_{\alpha\beta}(\omega) = \sum_n \frac{\langle \Psi_0^A | c_\alpha | \Psi_n^{A+1} \rangle \langle \Psi_n^{A+1} | c_\beta^\dagger | \Psi_0^A \rangle}{\hbar\omega - \varepsilon_n^+ + i\eta} + \sum_k \frac{\langle \Psi_0^A | c_\beta^\dagger | \Psi_k^{A-1} \rangle \langle \Psi_k^{A-1} | c_\alpha | \Psi_0^A \rangle}{\hbar\omega - \varepsilon_k^- - i\eta}$$

The reference state is a mean-field with only a few orbits





# The OpRS idea: Keep moments of the sp. fnct.

Original propagator: 
$$g_{\alpha\beta}(\omega) = \sum_n \frac{\langle \Psi_0^A | a_\alpha | \Psi_n^{A+1} \rangle \langle \Psi_n^{A+1} | a_\beta^\dagger | \Psi_0^A \rangle}{\hbar\omega - (E_n^{A+1} - E_0^A) + i\eta} + \sum_k \frac{\langle \Psi_0^A | a_\beta^\dagger | \Psi_k^{A-1} \rangle \langle \Psi_k^{A-1} | a_\alpha | \Psi_0^A \rangle}{\hbar\omega - (E_0^A - E_k^{A-1}) - i\eta}$$

OpRS approximation: 
$$g_{\alpha\beta}^{\text{OpRS}}(\omega) = \sum_{n \notin F} \frac{(\psi_\alpha^n)^* \psi_\beta^n}{\omega - \varepsilon_n^{\text{OpRS}} + i\eta} + \sum_{k \in F} \frac{\psi_\alpha^k (\psi_\beta^k)^*}{\omega - \varepsilon_k^{\text{OpRS}} - i\eta}$$

1st strategy: keep **particle** and **hole** distributions **separated**:

$$\tilde{M}_{\alpha\beta}^p = \sum_n (\chi_\alpha^n)^* \chi_\beta^n (\varepsilon_n^+)^p$$

$$\tilde{N}_{\alpha\beta}^p = \sum_k \gamma_\alpha^k (\gamma_\beta^k)^* (\varepsilon_k^-)^p,$$

$$M_{\alpha\beta}^{p,\text{OpRS}} = M_{\alpha\beta}^p, \quad p = 0, 1, 2, \dots, 2\kappa + 1$$

$$\kappa \geq 0$$

Koltun s.r. & 1-body observables fully retained:

$$\rho_{\alpha\beta} \equiv \langle \Psi_0^A | a_\beta^\dagger a_\alpha | \Psi_0^A \rangle = \int_{-\infty}^{\varepsilon_0^-} S_{\alpha\beta}^h(\omega) d\omega = \sum_k (\gamma_\beta^k)^* \gamma_\alpha^k$$

$$\langle \hat{O}^{1B} \rangle = \sum_{\alpha\beta} O_{\alpha\beta}^{1B} \rho_{\beta\alpha} = \sum_k \sum_{\alpha\beta} (\gamma_\alpha^k)^* O_{\alpha\beta}^{1B} \gamma_\beta^k$$

$$E_0^A = \sum_{\alpha\beta} \frac{1}{2} \int_{-\infty}^{\varepsilon_0^-} [T_{\alpha\beta} + \omega \delta_{\alpha\beta}] S_{\beta\alpha}^h(\omega) d\omega - \frac{1}{2} \langle \hat{W} \rangle$$

OpRS( $\kappa=0$ ) **has twice** the poles of a HF/MF





# The OpRS idea: Keep moments of the sp. fnct.

Original propagator: 
$$g_{\alpha\beta}(\omega) = \sum_n \frac{\langle \Psi_0^A | a_\alpha | \Psi_n^{A+1} \rangle \langle \Psi_n^{A+1} | a_\beta^\dagger | \Psi_0^A \rangle}{\hbar\omega - (E_n^{A+1} - E_0^A) + i\eta} + \sum_k \frac{\langle \Psi_0^A | a_\beta^\dagger | \Psi_k^{A-1} \rangle \langle \Psi_k^{A-1} | a_\alpha | \Psi_0^A \rangle}{\hbar\omega - (E_0^A - E_k^{A-1}) - i\eta}$$

OpRS approximation: 
$$g_{\alpha\beta}^{\text{OpRS}}(\omega) = \sum_{n \notin F} \frac{(\psi_\alpha^n)^* \psi_\beta^n}{\omega - \varepsilon_n^{\text{OpRS}} + i\eta} + \sum_{k \in F} \frac{\psi_\alpha^k (\psi_\beta^k)^*}{\omega - \varepsilon_k^{\text{OpRS}} - i\eta}$$

2nd strategy: group particle **and** hole distributions together:

$$M_{\alpha\beta}^p = \sum_n \frac{(\chi_\alpha^n)^* \chi_\beta^n}{[E_F - \varepsilon_n^+]^p} + \sum_k \frac{\gamma_\alpha^k (\gamma_\beta^k)^*}{[E_F - \varepsilon_k^-]^p}$$

Koltun s.r. & 1-body observables are still OK(-ish)

OpRS( $\kappa=0$ ) has same # of poles as HF/MF

$$M_{\alpha\beta}^{p, \text{OpRS}} = M_{\alpha\beta}^p, \quad p = 0, 1, 2, \dots, 2\kappa + 1$$

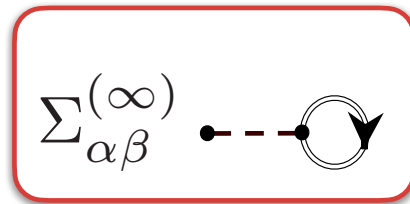
$$\kappa \geq 0$$



# The self-consistency loop (**approximated**)

Trial  
propagator:

$$g_{\alpha\beta}(\omega)$$



“sc $\kappa$ ” means approximating  
with OpRS( $\kappa$ ) but still iterating  
to self-consistency



# Linear response with SCGF

## some past works

F. Raimondi and CB, Phys. Rev. C**99**, 054327 (2019)  
CB and W. Dickhoff, Phys. Rev. C**68**, 014311 (2003)



# Dressed RPA

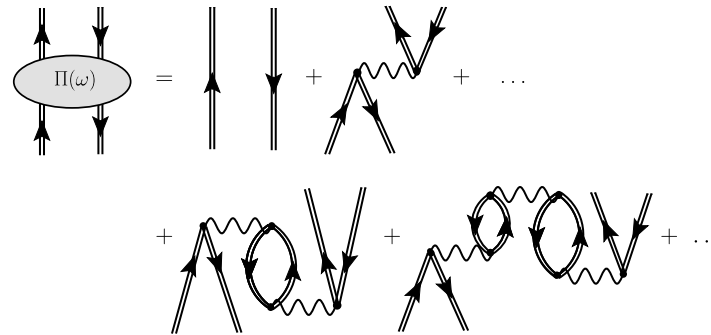
The Lehmann representation of the polarization propagator is

$$\Pi_{\gamma\delta,\alpha\beta}(\omega) = \sum_{n_\pi \neq 0} \frac{\langle \Psi_0^A | a_\delta^\dagger a_\gamma | \Psi_{n_\pi}^A \rangle \langle \Psi_{n_\pi}^A | a_\alpha^\dagger a_\beta | \Psi_0^A \rangle}{\hbar\omega - (E_{n_\pi}^A - E_0^A) + i\eta} - \sum_{n_\pi \neq 0} \frac{\langle \Psi_0^A | a_\alpha^\dagger a_\beta | \Psi_{n_\pi}^A \rangle \langle \Psi_{n_\pi}^A | a_\delta^\dagger a_\gamma | \Psi_0^A \rangle}{\hbar\omega + (E_{n_\pi}^A - E_0^A) - i\eta}, \quad (8)$$

DRPA uses the dressed propagator (or, better, the OpRS) and approximate  $K^{(ph)}=V$

The polarization propagator is the solution of the Bethe-Salpeter equation,

$$\Pi_{\gamma\delta,\alpha\beta}(\omega) = \Pi_{\gamma\delta,\alpha\beta}^f(\omega) + \sum_{\mu\rho\nu\sigma} \Pi_{\gamma\delta,\mu\rho}^f(\omega) \times K_{\mu\rho,\nu\sigma}^{(ph)}(\omega) \Pi_{\nu\sigma,\alpha\beta}(\omega), \quad (11)$$



Response observables are found as usual:

$$R(E) = -\frac{1}{\pi} \sum_{\substack{\alpha\beta \\ \gamma\delta}} \langle \gamma | \hat{Q}_{1m}^{T=1} | \delta \rangle^* \text{Im} \Pi_{\gamma\delta,\alpha\beta}(E) \langle \alpha | \hat{Q}_{1m}^{T=1} | \beta \rangle$$

**dipole response (E1)**

$$\sigma(E) = 4\pi^2 \alpha E R(E)$$

**Coulomb exit. X-section**

$$\alpha_D = 2\alpha \int dE \frac{R(E)}{E}$$

**dipole polarisability**



# Dressed RPA - sc0 with inverted poles

Isovector dipole response ( $N_{max}=13$ , NNLO<sub>sat</sub>, OpRS/sc0):

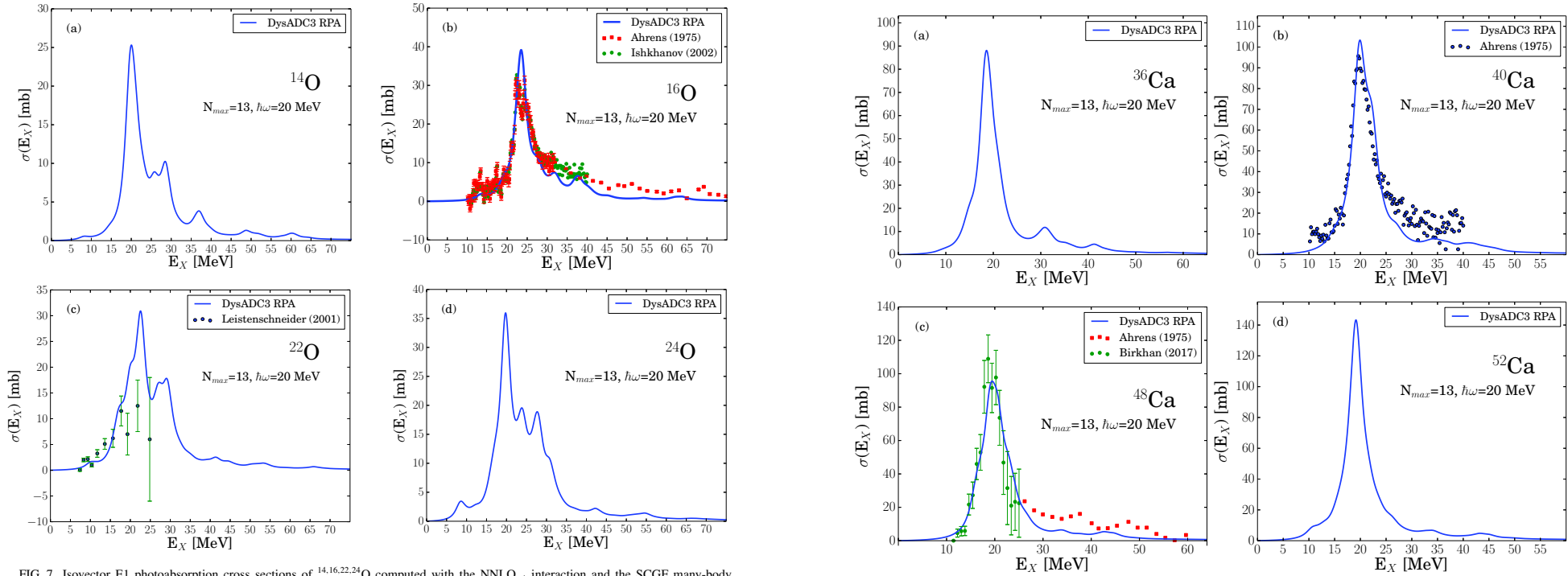
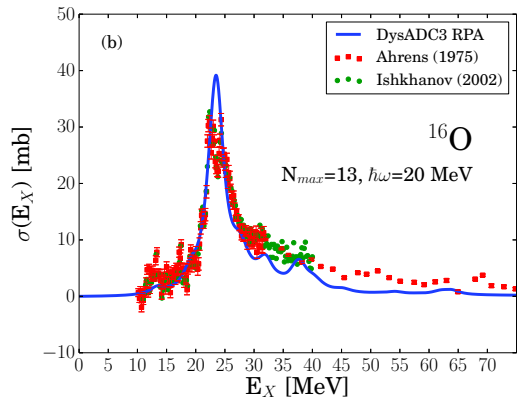


FIG. 7. Isovector E1 photoabsorption cross sections of  $^{14,16,22,24}\text{O}$  computed with the NNLO<sub>sat</sub> interaction and the SCGF many-body method. The reference  $g_{MP}^{\text{OpRS}}(\omega)$  propagator is computed using an ADC(3) self-energy. The curves are obtained by folding the discrete spectra with Lorentzian widths  $\Gamma = 3.0$  MeV. Experimental data for  $^{16}\text{O}$  in (b) are from Ahrens *et al.* [47] (red squares) and from Ishkhanov *et al.* [49] (green circles); experimental data for  $^{22}\text{O}$  in (c) are from Leistenschneider *et al.* [48].



# Dressed RPA - dependence on the choice of OpRS



“Inverse poles” OpRS(k=0)

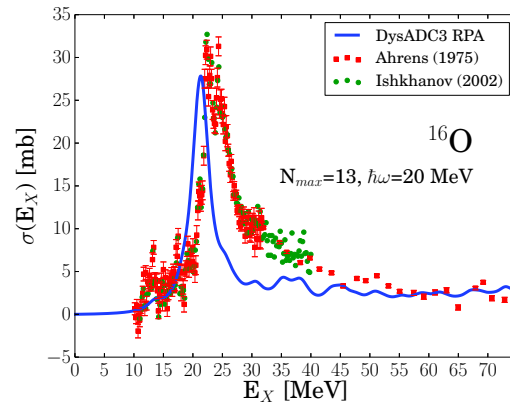
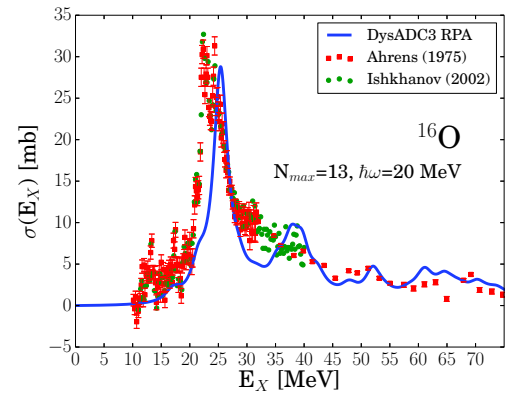


FIG. 11. Same as Fig. 10 but with  $\tilde{\rho}_{p \leq 3}^{\text{OpRS}}(\omega)$ .

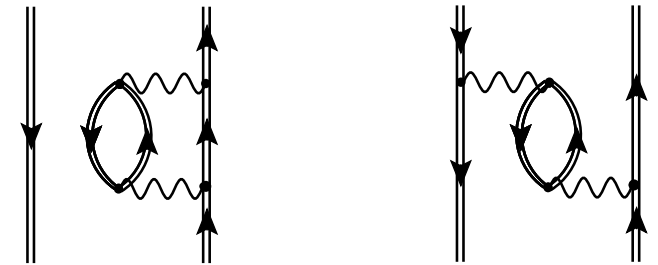


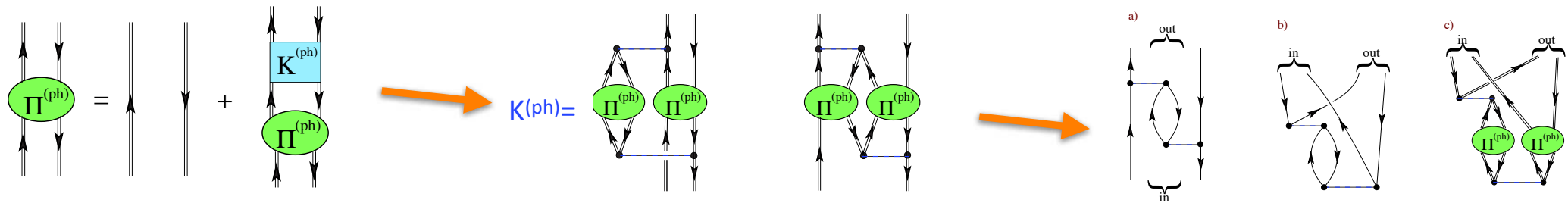
FIG. 2. Example of diagrams contributing to the  $ph$  polarization propagator  $\Pi(\omega)$  with  $2p2h$  intermediate configurations. (Left) Non-interacting  $1h + 2p1h$  terms that contribute to DRPA through the dressing of the reference propagator. (Right) Interaction among the  $ph$  pair mediated by a phonon exchange.

“Direct poles” OpRS(k=0,1)

FIG. 10. Photoabsorption cross sections of  $^{16}\text{O}$  computed with  $\tilde{\rho}_{p \leq 3}^{\text{OpRS}}(\omega)$ . The computed DRPA spectrum is convoluted with a Lorentzian width of  $\Gamma = 3.0$  MeV. Experimental data are from Ahrens *et al.* [47] (red squares) and from Ishkhanov *et al.* [49] (green circles).

# Extending DRPA to double phonons

Follows the FRPA/ADC(n) strategy:



$$\Pi_{\gamma\delta,\alpha\beta}(\omega) = \Pi_{\gamma\delta,\alpha\beta}^f(\omega) + \sum_{\mu\rho\nu\sigma} \Pi_{\gamma\delta,\mu\rho}^f(\omega) \times K_{\mu\rho,\nu\sigma}^{(ph)}(\omega) \Pi_{\nu\sigma,\alpha\beta}(\omega),$$

$$\Pi^f(\omega) \rightarrow \Pi^{f>}(\omega) + \Pi^{f<}(\omega)$$

$$\Pi(\omega) \rightarrow \Pi^{>}(\omega) + \Pi^{<}(\omega)$$

$$\Pi^{>}(\omega) = \Pi^{f>}(\omega) + \Pi^{f>}(\omega) \{ [V + W^{>}(\omega)] \Pi^{>}(\omega) + (V + H^{>,<}) \Pi^{<}(\omega) \},$$

$$\Pi^{<}(\omega) = \Pi^{f<}(\omega) + \Pi^{f<}(\omega) \{ (V + H^{<,>}) \Pi^{>}(\omega) + [V + W^{<}(\omega)] \Pi^{<}(\omega) \}.$$

$$\omega \begin{pmatrix} X^{(1)} \\ X^{(2)} \\ Y^{(1)} \\ Y^{(2)} \end{pmatrix} = \mathbf{M} \begin{pmatrix} X^{(1)} \\ X^{(2)} \\ Y^{(1)} \\ Y^{(2)} \end{pmatrix}$$

$$\mathbf{M} = \begin{bmatrix} GV & G^\dagger + D & GK^{>\dagger} & G[V + H^{>,<}] (G^*)^\dagger \\ K^{>} G^\dagger & E & & \\ -G^* [V + H^{<,>}] G^\dagger & & -G^* V (G^*)^\dagger - D & G^* K^{<\dagger} \\ & & K^{<} (G^*)^\dagger & -E \end{bmatrix}$$



# Extending DRPA to double phonons (results for oxygen)

Choice of IPM vs. “OpRS” propagators

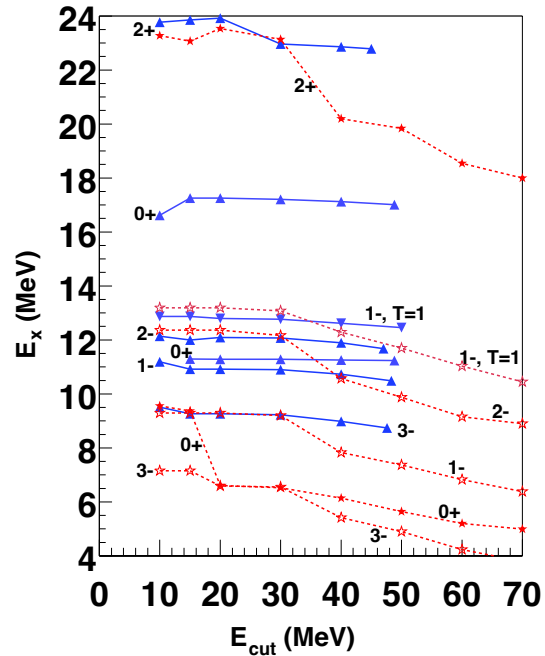


FIG. 7. Dependence of the ERPA solutions on the number of two-phonon states considered. For any given point, all the configuration with energy  $\varepsilon_{n_a}^\pi + \varepsilon_{n_b}^\pi \leq E_{cut}$  have been included in the calculation. Solid (dashed) lines refer to the results obtained from a dressed (IPM) input propagator.

“Ab initio” Double phonons not explaining low-lying 0+ (but explaining other things):

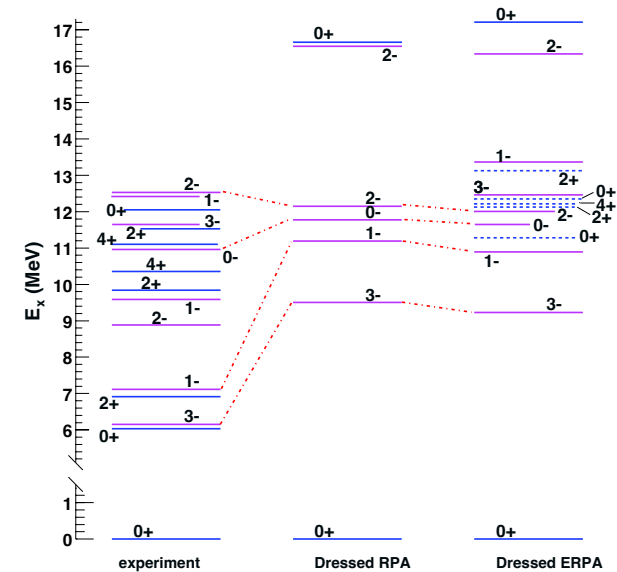


FIG. 6. Results for the DRPA and the two-phonon ERPA propagator of  $^{16}\text{O}$  with a dressed input propagator from Ref. [9], middle, and last column, respectively. In solving the ERPA equation, the lowest  $3^-$ ,  $1^-$ , and  $0^+$  levels of the DRPA propagator were shifted to their experimental energies. All other DRPA solutions were left unchanged. The excited states indicated by dashed lines are those for which the (E)RPA equation predicts a total spectral strength  $Z_{n_\pi}$  lower than 10%. The first column reports the experimental results [44].





# Ab initio optical potentials from propagator theory

## Relation to Feshbach theory:

Mahaux & Sartor, Adv. Nucl. Phys. 20 (1991)

Escher & Jennings Phys. Rev. C66, 034313 (2002)

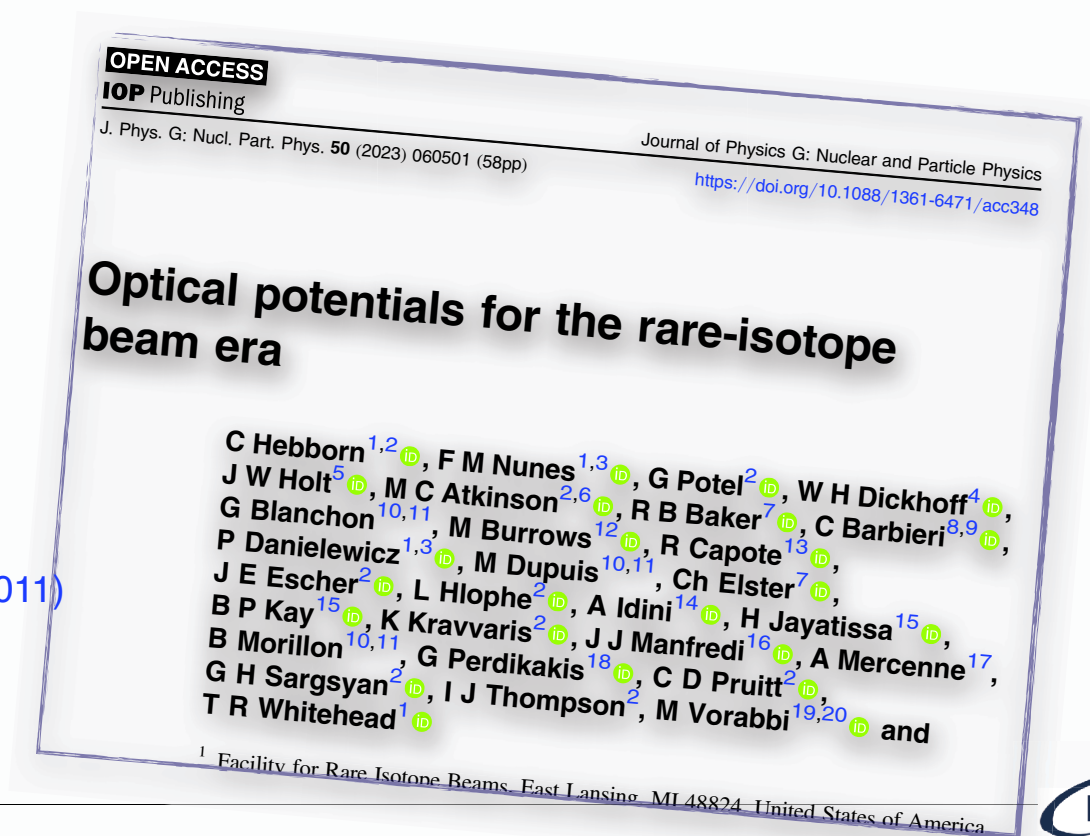
## Previous SCGF work:

CB, B. Jennings, Phys. Rev. C72, 014613 (2005)

S. Waldecker, CB, W. Dickhoff, Phys. Rev. C84, 034616 (2011)

A. Idini, CB, P. Navrátil, Phys. Rv. Lett. 123, 092501 (2019)

M. Vorabbi, CB, et al., in preparation



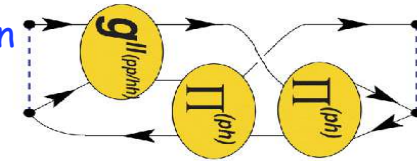
# Microscopic optical potential

Nuclear self-energy  $\Sigma^*(\mathbf{r}, \mathbf{r}'; \varepsilon)$ :

- contains **both particle** and **hole** props.
- it is proven to be a **Feshbach opt. pot**  $\rightarrow$  in general it is **non-local** !

$$\Sigma_{\alpha\beta}^*(\omega) = \underbrace{\Sigma_{\alpha\beta}^{(\infty)} + \sum_{i,j} \mathbf{M}_{\alpha,i}^\dagger \left( \frac{1}{E - (\mathbf{K}^> + \mathbf{C}) + i\Gamma} \right)_{i,j} \mathbf{M}_{j,\beta}}_{\text{mean-field}} + \sum_{r,s} \mathbf{N}_{\alpha,r} \left( \frac{1}{E - (\mathbf{K}^< + \mathbf{D}) - i\Gamma} \right)_{r,s} \mathbf{N}_{s,\beta}^\dagger$$

Particle-vibration couplings:



Solve scattering and overlap functions directly in momentum space:

$$\Sigma^{*l,j}(k, k'; E) = \sum_{n, n'} R_{nl}(k) \Sigma_{n, n'}^{*l,j} R_{nl}(k')$$

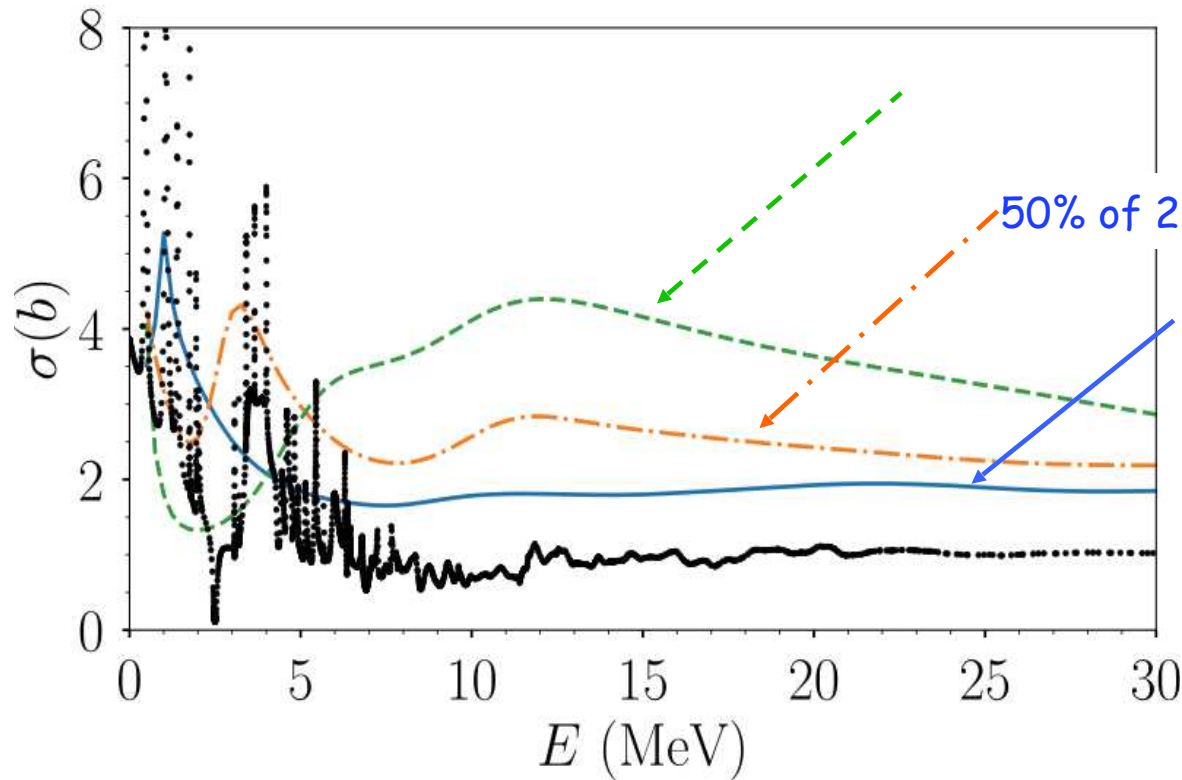
$$\frac{k^2}{2\mu} \psi_{l,j}(k) + \int dk' k'^2 \Sigma^{*l,j}(k, k'; E_{c.m.}) \psi_{l,j}(k') = E_{c.m.} \psi_{l,j}(k)$$



# Role of intermediate state configurations (ISCs)

$n\text{-}^{16}\text{O}$ , total elastic cross section

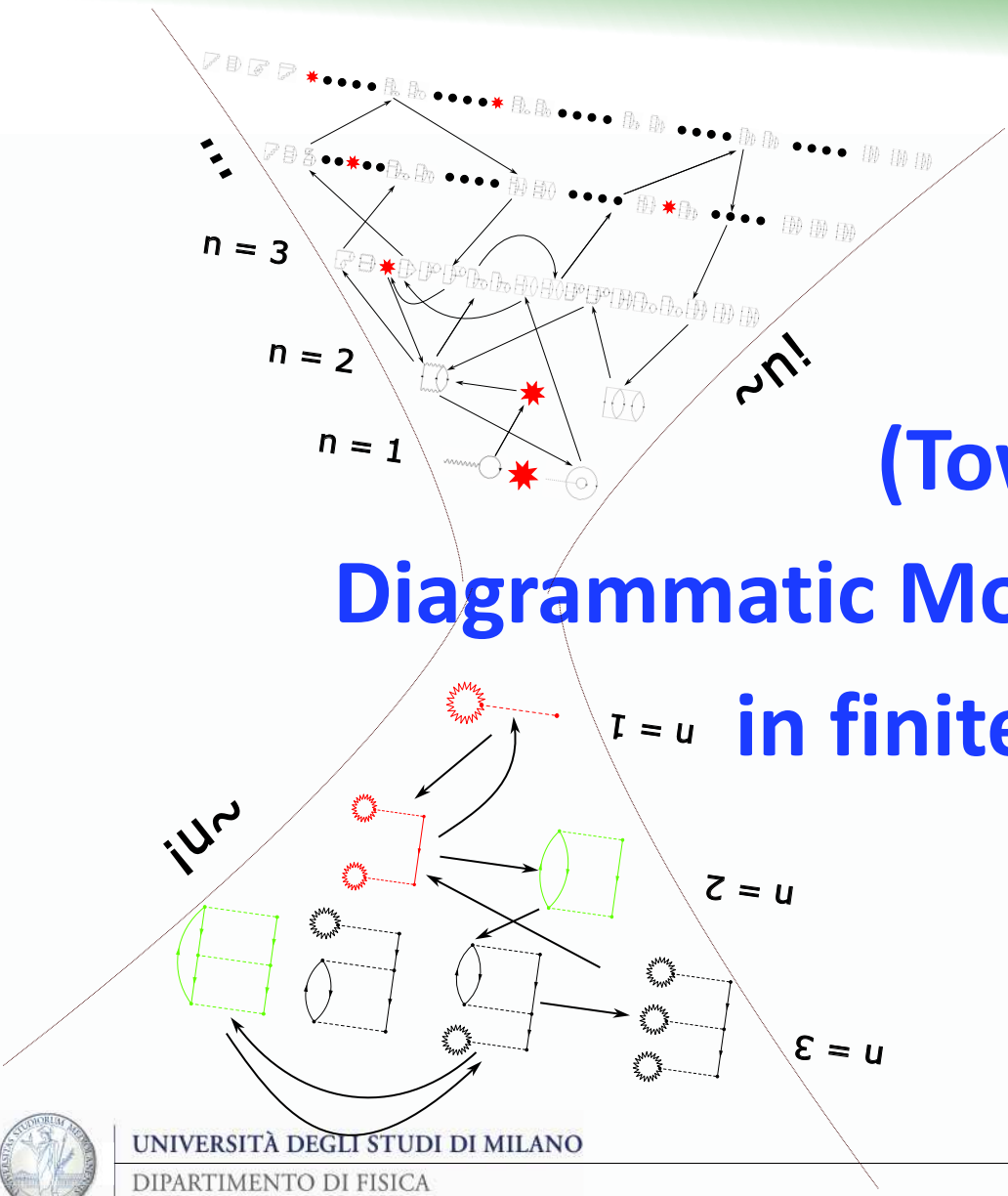
[A. Idini, CB, Navrátil,  
Phys. Rev. Lett. **123**, 092501 (2019)]



High order configurations, or  
ADC( $n > 3$ ), to be critical for fully  
ab initio optical potentials

$$\Sigma_{\alpha\beta}^*(\omega) = \Sigma_{\alpha\beta}^{(\infty)} + \sum_{i,j} \mathbf{M}_{\alpha,i}^\dagger \left( \frac{1}{E - (\mathbf{K}^> + \mathbf{C}) + i\Gamma} \right)_{i,j} \mathbf{M}_{j,\beta} + \sum_{r,s} \mathbf{N}_{\alpha,r} \left( \frac{1}{E - (\mathbf{K}^< + \mathbf{D}) - i\Gamma} \right)_{r,s} \mathbf{N}_{s,\beta}^\dagger$$





**(Toward)**  
**Diagrammatic Monte Carlo (DiagMC)**  
**in finite systems**



S. Brolli  
 (Masters thesis)

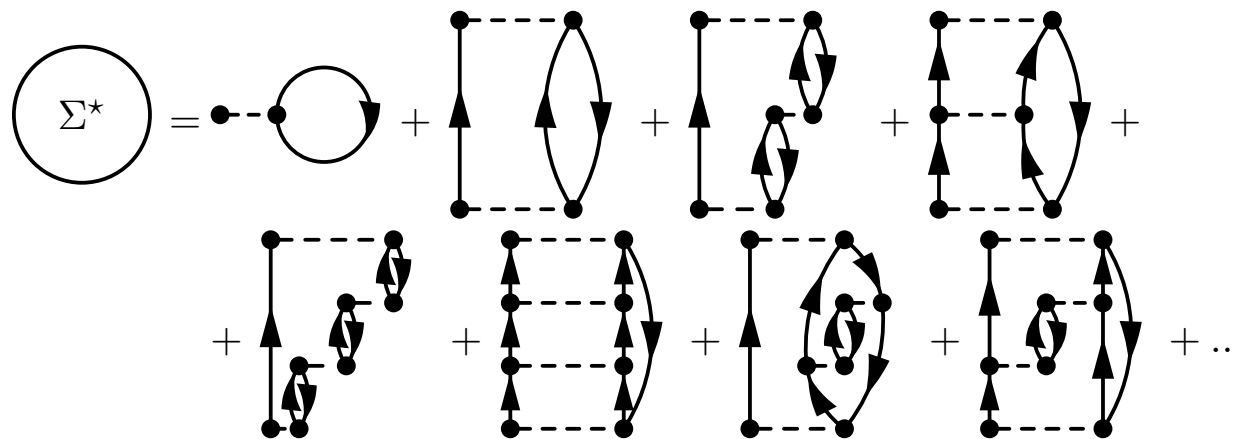


# Green's function theory **beyond ADC(3)?**

The Green's function is found as the exact solution of the Dyson equation:

$$G_{\alpha\beta}(\omega) = G_{\alpha\beta}^{(0)}(\omega) + \sum_{\gamma\delta} G_{\alpha\gamma}^{(0)}(\omega) \Sigma_{\gamma\delta}^*(\omega) G_{\delta\beta}(\omega)$$

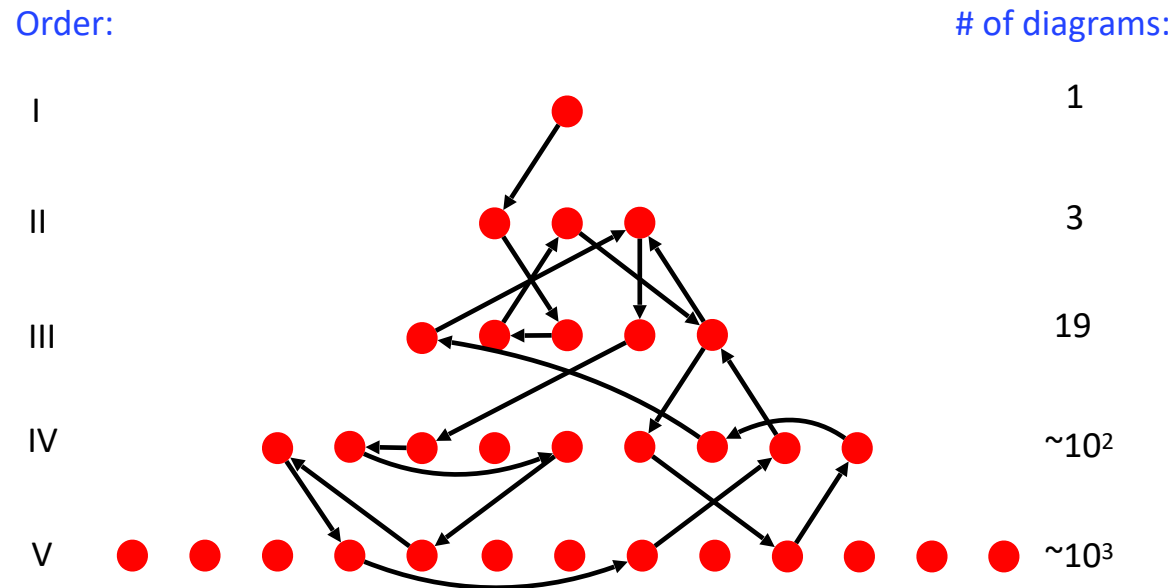
It requires knowing the self-energy which is the sum of an *infinite series* of Feynman diagrams:



The number of required diagrams explodes (factorially!) with the order of the approximation...

Diagrams grow factorially (more than exponentially) with the order

A direct calculation of all diagrams beyond order three is unfeasible.



Diagrammatic Monte Carlo (DiagMC) *samples diagrams in their topological space* using a Markov chain.



# Diagrammatic Monte Carlo: overview

S. Brolli (Masters thesis)

$$\Sigma_{\alpha\beta}^*(\omega) = \sum_{\mathcal{T}} \sum_{\gamma_1 \dots \gamma_n} \int d\omega_1 \dots d\omega_m \mathcal{D}_{\alpha\beta}^\omega(\mathcal{T}; \gamma_1 \dots \gamma_n; \omega_1 \dots \omega_m) 1_{\mathcal{T} \in \mathcal{S}_{\Sigma^*}}$$

We define  $\mathcal{C} := (\mathcal{T}; \gamma_1 \dots \gamma_n; \omega_1 \dots \omega_m)$

$$\Sigma_{\alpha\beta}^*(\omega) = \int d\mathcal{C} |\mathcal{D}_{\alpha\beta}^\omega(\mathcal{C})| e^{i \arg[\mathcal{D}_{\alpha\beta}^\omega(\mathcal{C})]} 1_{\mathcal{T} \in \mathcal{S}_{\Sigma^*}}$$

$$\Sigma_{\alpha\beta}^*(\omega) = Z_{\alpha\beta}^\omega \int d\mathcal{C} \frac{|\mathcal{D}_{\alpha\beta}^\omega(\mathcal{C})| W_o(N)}{Z_{\alpha\beta}^\omega} \frac{e^{i \arg[\mathcal{D}_{\alpha\beta}^\omega(\mathcal{C})]} W_o(N)}{W_o(N)} 1_{\mathcal{T} \in \mathcal{S}_{\Sigma^*}}$$

- $W_o(N)$  is an order dependent reweighting factor
- $Z_{\alpha\beta}^\omega = \int d\mathcal{C} |\mathcal{D}_{\alpha\beta}^\omega(\mathcal{C})| W_o(N)$  is a normalization factor
- $w_{\alpha\beta}^\omega(\mathcal{C}) := \frac{|\mathcal{D}_{\alpha\beta}^\omega(\mathcal{C})| W_o(N)}{Z_{\alpha\beta}^\omega}$  is a probability distribution function



# Diagrammatic Monte Carlo: normalization

The Markov chain must have the correct equilibrium distribution  $w_{\alpha\beta}^{\omega}(\mathcal{C})$ :

$$\Sigma_{\alpha\beta}^*(\omega) = Z_{\alpha\beta}^{\omega} \left[ \lim_{n \rightarrow \infty} \frac{1}{n} \sum_{i=1}^n \frac{e^{i \arg[\mathcal{D}_{\alpha\beta}^{\omega}(\mathcal{C}_i)]}}{W_o(N)} 1_{\mathcal{T}_i \in \mathcal{S}_{\Sigma^*}} \right]$$

where the normalization  $Z_{\alpha\beta}^{\omega}$  is unknown but it can be estimated.

We turn propagators that close on themselves into zigzag lines with an arbitrary value

$$e^{i\omega_1 \eta} G_{\alpha}(\omega_1) = \frac{\alpha}{\alpha} \text{ (loop) } \omega_1 \longrightarrow \frac{\alpha}{\alpha} \text{ (zigzag) } \omega_1 := -ie^{-k\omega_1^2}$$

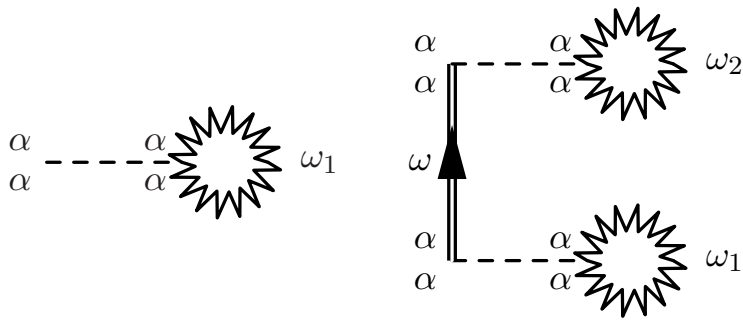
with  $k$  an arbitrary constant that can be used to optimize the convergence.





# Diagrammatic Monte Carlo: normalization

Define the normalisation sector  $\mathcal{S}_N$  to be made of *both* these diagrams:



- These diagrams belong to  $w_\alpha^\omega$  but not to  $\mathcal{S}_{\Sigma^*}$
- They are easy to integrate and to simulate with the Monte Carlo method

$\mathcal{S}_N$  has weight:

$$\mathcal{Z}_{N\alpha}^\omega := \int_{\mathcal{S}_N} d\mathcal{C} w_\alpha^\omega = \frac{|g|}{4\sqrt{\pi k}} + \frac{g^2}{16\pi k} |G_\alpha(\omega)| W_o(2)$$

The expected number of times the normalization sector is visited ( $\mathcal{N}$ ) gives the normalization  $\mathcal{Z}_\alpha^\omega$ :

$$\frac{\mathcal{Z}_{N\alpha}^\omega}{\mathcal{Z}_\alpha^\omega} = \lim_{n \rightarrow \infty} \frac{\mathcal{N}}{n}$$

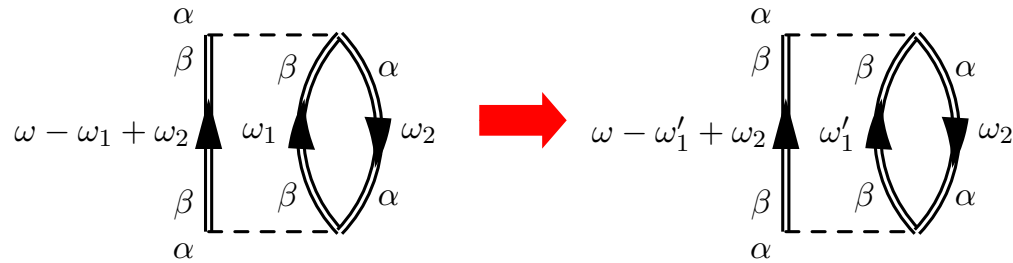
Then, we get the fundamental equation of DiagMC:  $\Sigma_\alpha^*(\omega) = \mathcal{Z}_{N\alpha}^\omega \lim_{n \rightarrow \infty} \frac{1}{\mathcal{N}} \sum_{i=1}^n \frac{e^{i \arg[\mathcal{D}_\alpha^\omega(\mathcal{C}_i)]}}{W_o(N)} 1_{\mathcal{T}_i \in \mathcal{S}_{\Sigma^*}}$



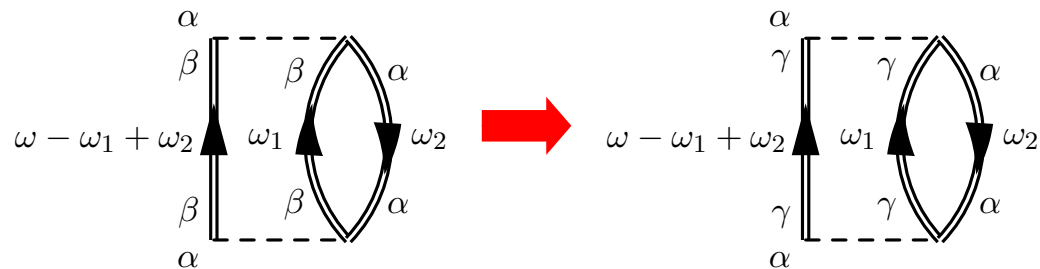
# The updates

- 1 Change Frequency
  - 2 Change Single-Particle Quantum Numbers
- } Standard Monte Carlo

*Change Frequency:*



*Change Single-Particle Quantum Numbers:*

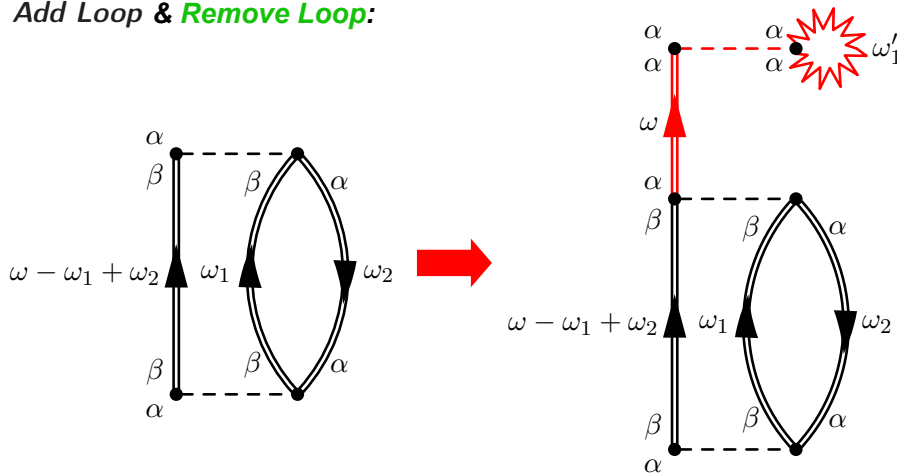


# The updates

S. Brolli (Masters thesis)

- 3 Add Loop
  - 4 Remove Loop
  - 5 Reconnect
- } Monte Carlo on the topology

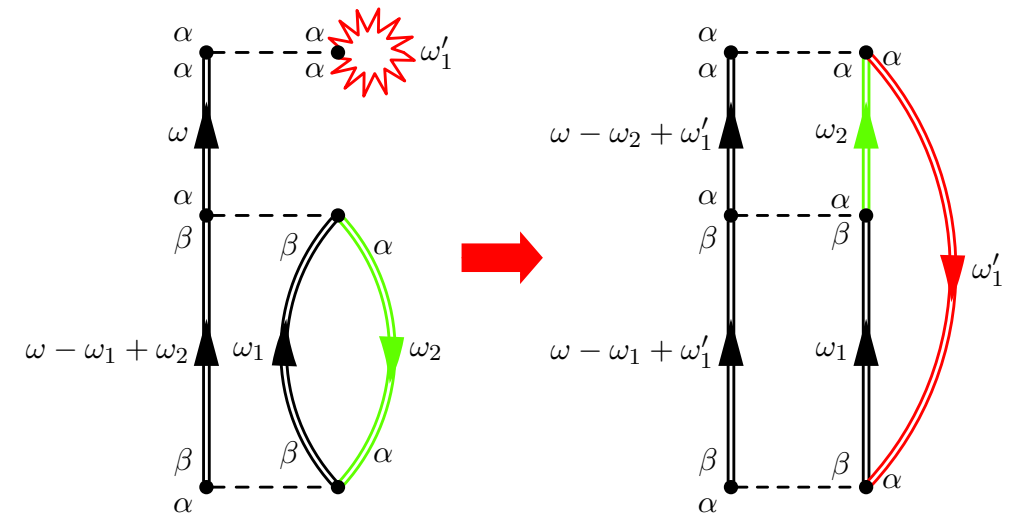
Add Loop & Remove Loop:



$\omega'_1$  is drawn from the probability distribution  $W_f(\omega'_1)$ .

$$q_{AL} = \frac{|g|}{4\pi} \frac{1}{W_f(\omega'_1)} e^{-k\omega_1'^2} |G_\alpha(\omega)| \frac{W_o(3)}{W_o(2)}$$

Reconnect:

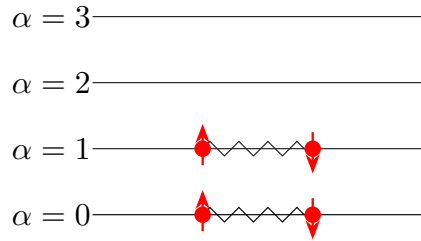


The unphysical propagators are turned into physical ones when reconnected.



# Results of the simulation for D=4

$$H = \xi \sum_{\alpha=0}^{D-1} \sum_{\sigma=+,-} \alpha c_{\alpha\sigma}^\dagger c_{\alpha\sigma} - \frac{g}{2} \sum_{\alpha,\beta=0}^{D-1} c_{\alpha+}^\dagger c_{\alpha-}^\dagger c_{\beta-} c_{\beta+}$$



$$\Sigma_{\alpha\beta}^*(\omega) = \Sigma_{\alpha\beta}^{(\infty)} + \sum_{i,j} \mathbf{M}_{\alpha,i}^\dagger \left( \frac{1}{E - (\mathbf{K}^> + \mathbf{C}) + i\Gamma} \right)_{i,j} \mathbf{M}_{j,\beta} + \sum_{r,s} \mathbf{N}_{\alpha,r} \left( \frac{1}{E - (\mathbf{K}^< + \mathbf{D}) - i\Gamma} \right)_{r,s} \mathbf{N}_{s,\beta}^\dagger$$

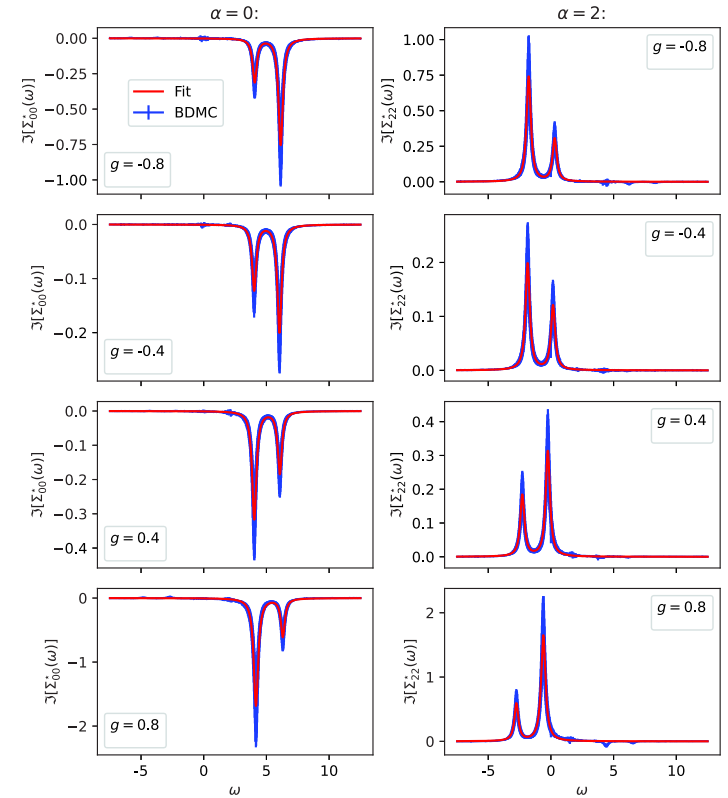
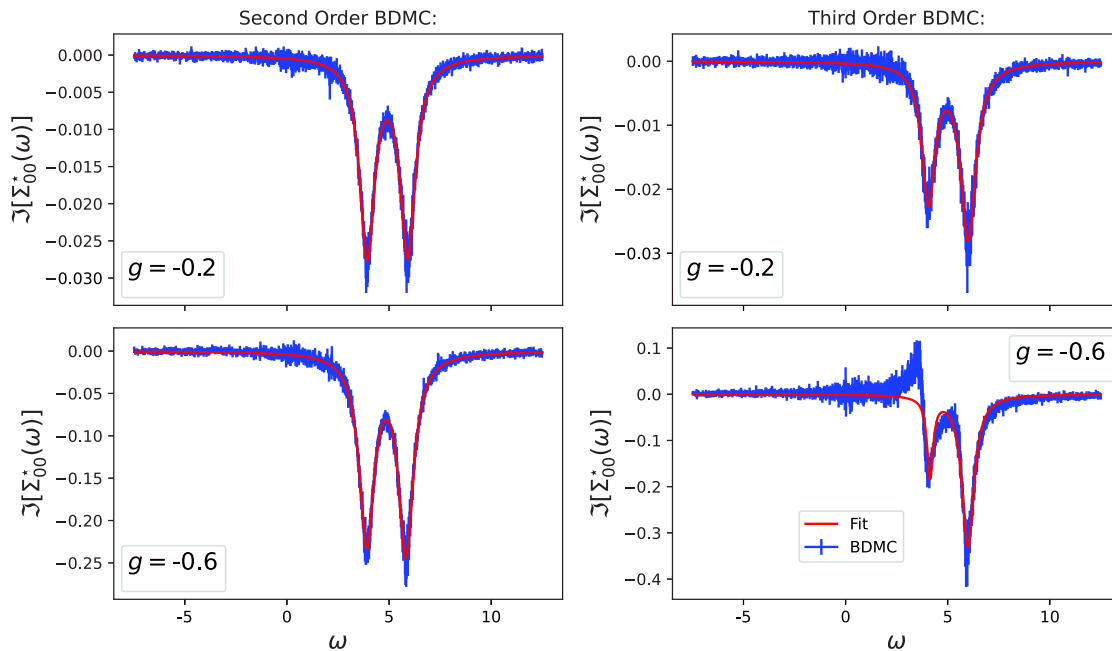


Figure 4.1: Components  $\alpha = 0$  and  $\alpha = 2$  of the imaginary part of the self-energy for different values of the coupling  $g$ . The blue line is the results obtained with the BDMC simulation, while the red line is the best fit as a sum of two Lorentzians. The results for the two values of  $\alpha = 0, 2$  are displayed respectively on the left and on the right of the graph. The error bars are calculated as explained in the main text.



# Results of the simulation for D=4

Imaginary part of the component  $\alpha = 0$  of the diagonal **self-energy** for different values of the coupling:



$$H = \xi \sum_{\alpha=0}^{D-1} \sum_{\sigma=+,-} \alpha c_{\alpha\sigma}^\dagger c_{\alpha\sigma} - \frac{g}{2} \sum_{\alpha,\beta=0}^{D-1} c_{\alpha+}^\dagger c_{\alpha-}^\dagger c_{\beta-} c_{\beta+}$$

We fitted the imaginary part of the self-energy as a sum of Lorentzians.

S. Brolli, CB, Vigezzi,  
in preparation

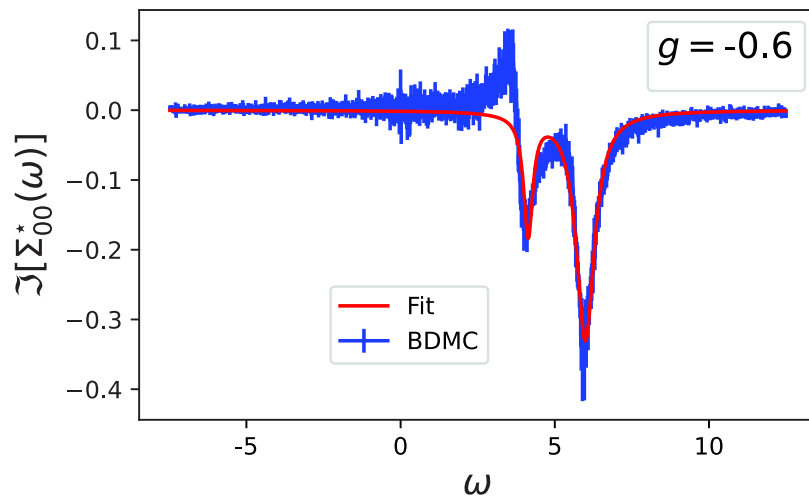


# Reorganization in terms of ladders ( $\Gamma$ )

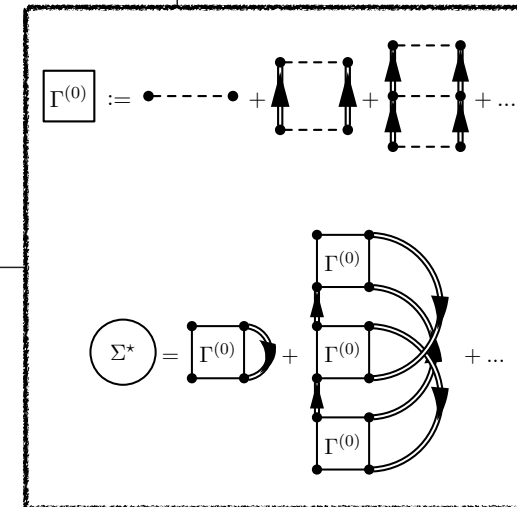
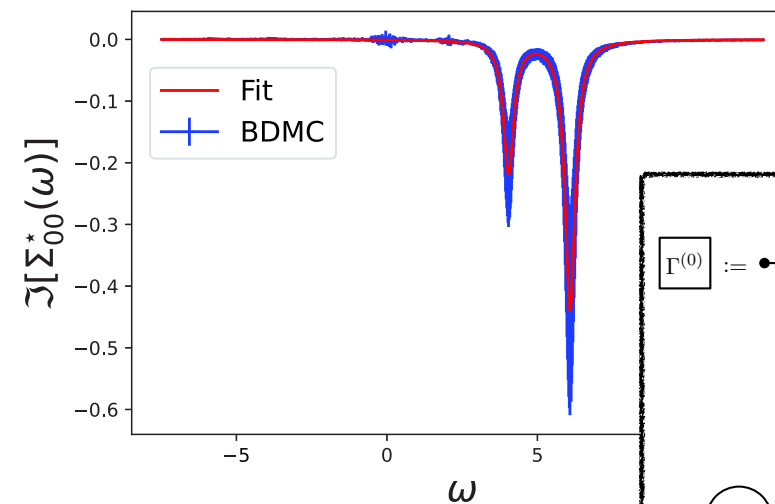
S. Brolli, CB, Vigezzi,  
in preparation

Imaginary part of the component  $\alpha=0$  of the diagonal self-energy ( $g=-0.6$ ):

Old updating scheme:



New updating scheme:

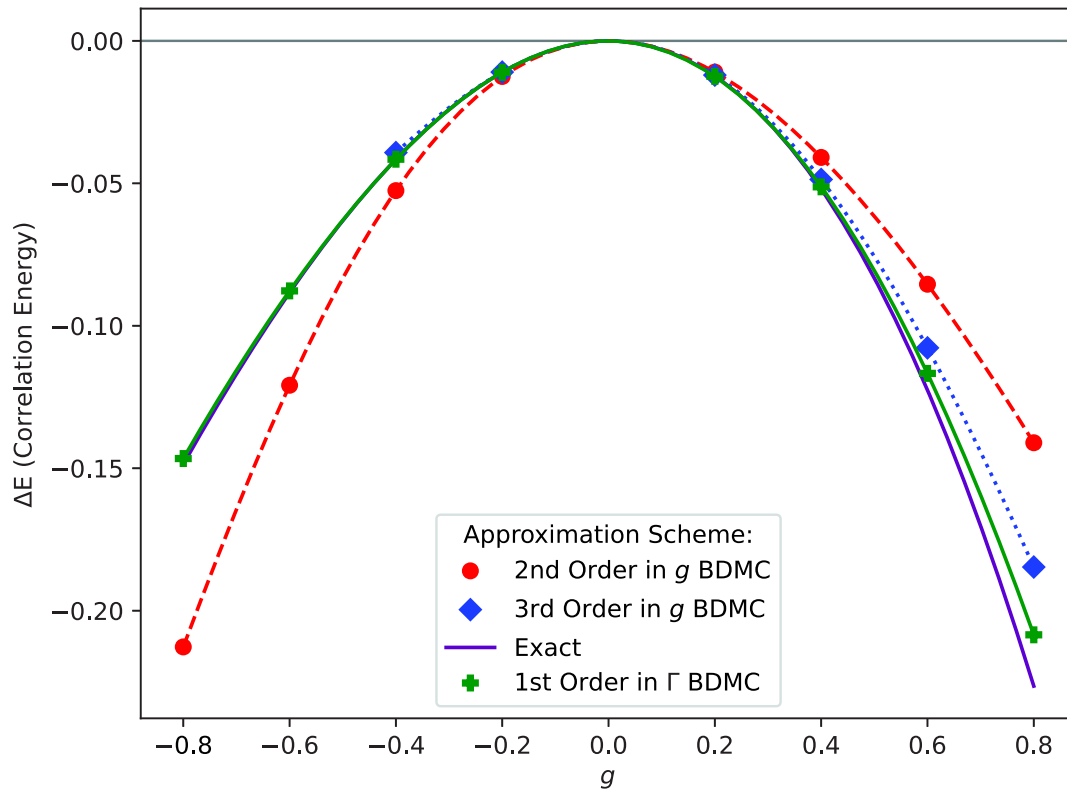


It restores the correct spectral representation also for  $g < -0.4$ !

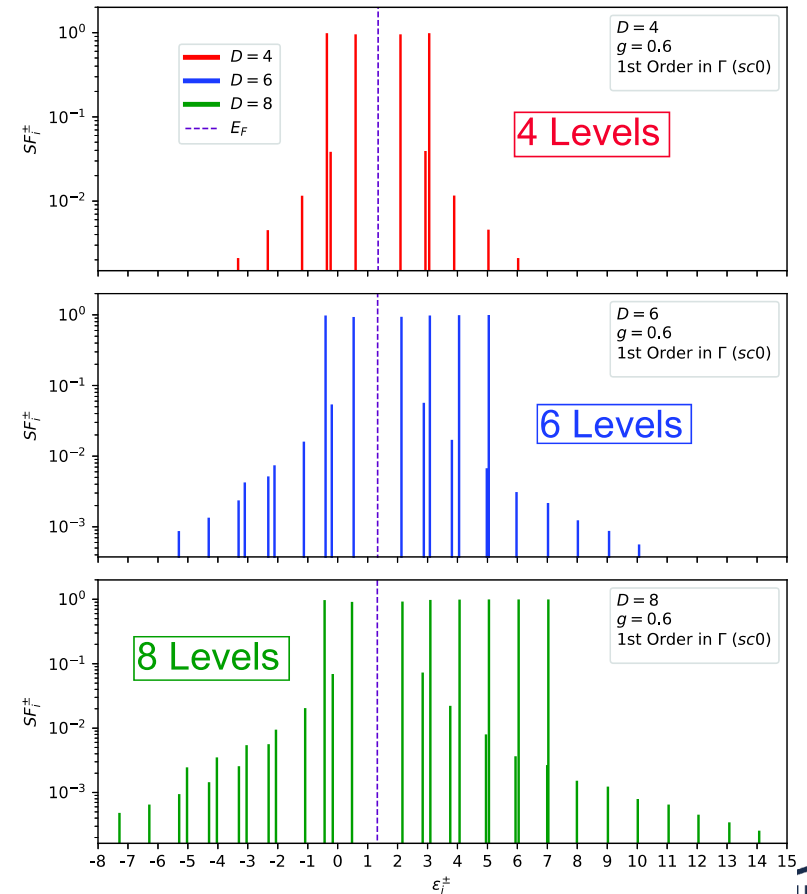


# Reorganization in terms of ladders ( $\Gamma$ )

Correlation energy  $\Delta E = E - E_{HF}$  as a function of interaction strength ( $g$ ):



Spectroscopic function for different dimensions of the model space ( $D$ ):



# SCGF computations of infinite matter



*F. Marino (PhD Thesis)*











# Nuclear Density Functional from Ab Initio Theory

PHYSICAL REVIEW C **104**, 024315 (2021)

## Nuclear energy density functionals grounded in *ab initio* calculations

F. Marino <sup>1,2,\*</sup> C. Barbieri <sup>1,2</sup> A. Carbone,<sup>3</sup> G. Colò <sup>1,2</sup> A. Lovato <sup>4,5</sup> F. Pederiva,<sup>6,5</sup> X. Roca-Maza <sup>1,2</sup>  
and E. Vigezzi <sup>2</sup>

<sup>1</sup>Dipartimento di Fisica “Aldo Pontremoli,” Università degli Studi di Milano, 20133 Milano, Italy

<sup>2</sup>Istituto Nazionale di Fisica Nucleare, Sezione di Milano, 20133 Milano, Italy

<sup>3</sup>Istituto Nazionale di Fisica Nucleare—CNAF, Viale Carlo Rortti Pichat 6/2, 40127 Bologna, Italy

DFT is in principle exact – but the energy density functional (EDF) is not known

For nuclear physics this is even more demanding: need to link the EDF to theories rooted in QCD!

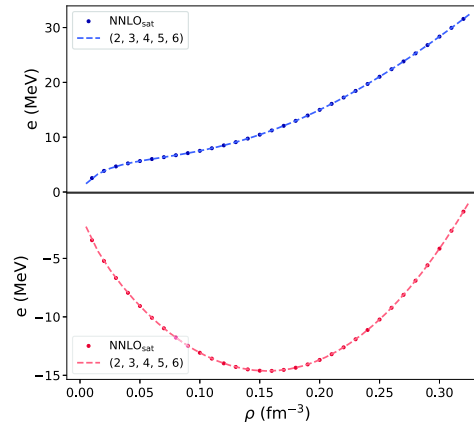
*Machine-learn DFT functional on the nuclear equation of state*

Jacob’s ladder



+ approximate GA

Benchmark in finite systems



$$E = \int d\mathbf{r} \mathcal{E}(\mathbf{r}) = E_{\text{kin}} + E_{\text{pot}} + E_{\text{Coul}}$$

$$E_{\text{GA}} = E_{\text{LDA}} + E_{\text{surf}}$$

$$E_{\text{surf}} = \int d\mathbf{r} \left[ \sum_{t=0,1} C_t^\Delta \rho_t \Delta \rho_t - \frac{W_0}{2} \left( \rho \nabla \cdot \mathbf{J} + \sum_q \rho_q \nabla \cdot \mathbf{J}_q \right) \right]$$



# Benchmark on finite systems

Machine-learn DFT functional  
on the nuclear equation of state

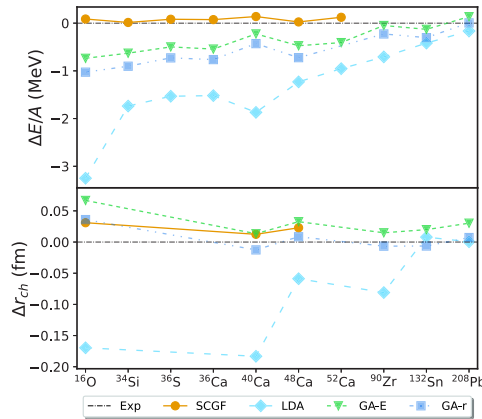
Jacob's ladder



+ approximate GA

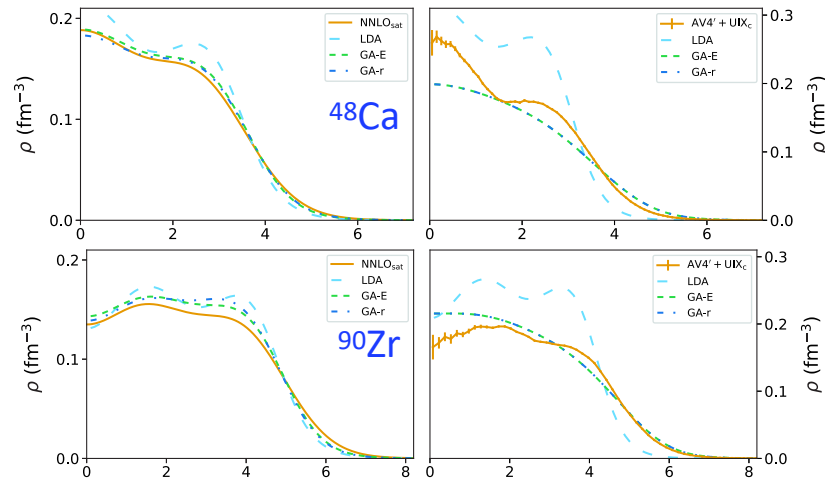
Benchmark in finite systems

Gradient terms are important (but they seem to work!):



SCGF/NNLO-sat :

AFDMC/AV4' :



Need to extract gradient information  
from non-uniform matter



External (monochromatic)  
perturbation:

$$v(\mathbf{x}) = v_q e^{i\mathbf{q}\cdot\mathbf{x}} + c.c. = 2v_q \cos(\mathbf{q}\cdot\mathbf{x})$$

$$\delta\rho(\mathbf{x}) = 2\rho_q \cos(\mathbf{q}\cdot\mathbf{x})$$



# ADC(3) computations for infinite matter

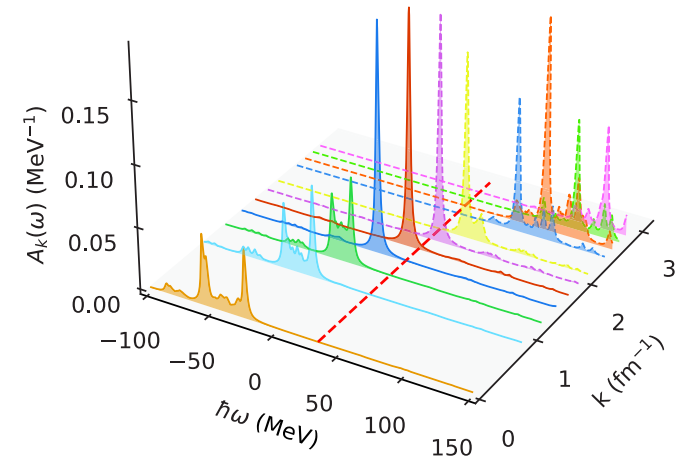
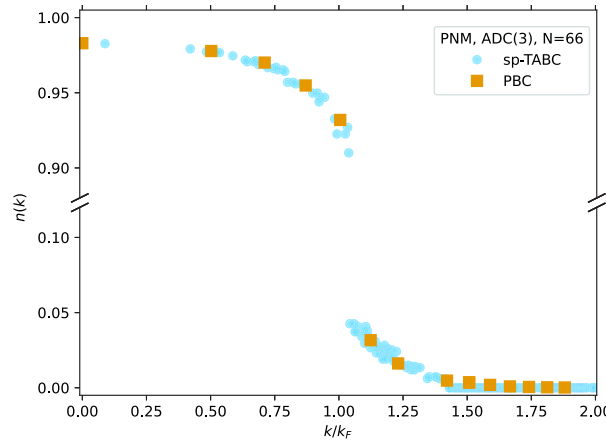
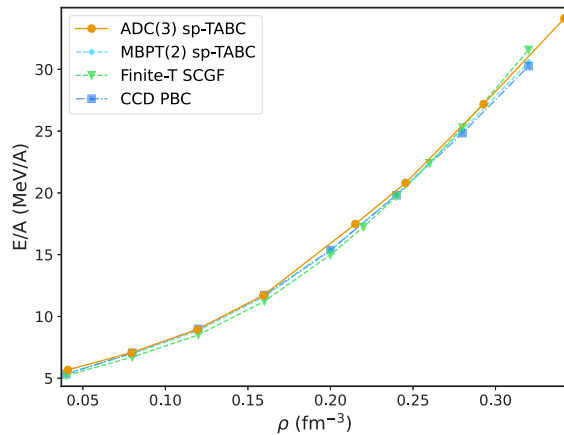
Finite size box (of length L) with periodic boundary conditions:

$$\rho = \frac{A}{L^3} \quad p_F = \sqrt[3]{\frac{6\pi^2\rho}{v_d}}$$

$$\phi(x + L, y, z) = \phi(x, y, z)$$

...

A=66, 2+3 NF (NNLOsat)



$$\hat{H} = \sum_{\alpha} \varepsilon_{\alpha}^0 a_{\alpha}^{\dagger} a_{\alpha} - \sum_{\alpha\beta} U_{\alpha\beta} a_{\alpha}^{\dagger} a_{\beta} + \frac{1}{4} \sum_{\substack{\alpha\gamma \\ \beta\delta}} V_{\alpha\gamma,\beta\delta} a_{\alpha}^{\dagger} a_{\gamma}^{\dagger} a_{\delta} a_{\beta} + \frac{1}{36} \sum_{\substack{\alpha\gamma\epsilon \\ \beta\delta\eta}} W_{\alpha\gamma\epsilon,\beta\delta\eta} a_{\alpha}^{\dagger} a_{\gamma}^{\dagger} a_{\epsilon}^{\dagger} a_{\eta} a_{\delta} a_{\beta}.$$

ADC(3) self energy:

$$\Sigma_{\alpha\beta}^{(*)}(\omega) = -U_{\alpha\beta} + \Sigma_{\alpha\beta}^{(\infty)} + M_{\alpha,r}^{\dagger} \left[ \frac{1}{\omega - [E^{>} + C]_{r,r'} + i\eta} \right]_{r,r'} M_{r',\beta} + N_{\alpha,s} \left[ \frac{1}{\omega - (E^{<} + D) - i\eta} \right]_{s,s'} N_{s',\beta}^{\dagger}$$



# Combined Gkv-ADC(1) + Dys ADC(3)

- Self energy:

$$\Sigma_{\alpha\beta}^* g_1 g_2(\omega) = \underbrace{\Sigma_{\alpha\beta}^{(\infty)} g_1 g_2}_{\text{Gorkov-ADC(1)}} + M_{\alpha}^{\dagger} \left[ \frac{1}{\omega - E^{2p1h} + i\eta} \right] M_{\beta} + N_{\alpha} \left[ \frac{1}{\omega - E^{2h1p} - i\eta} \right] N_{\beta}^{\dagger}$$

Dyson-ADC(3)  
(only normal part!)

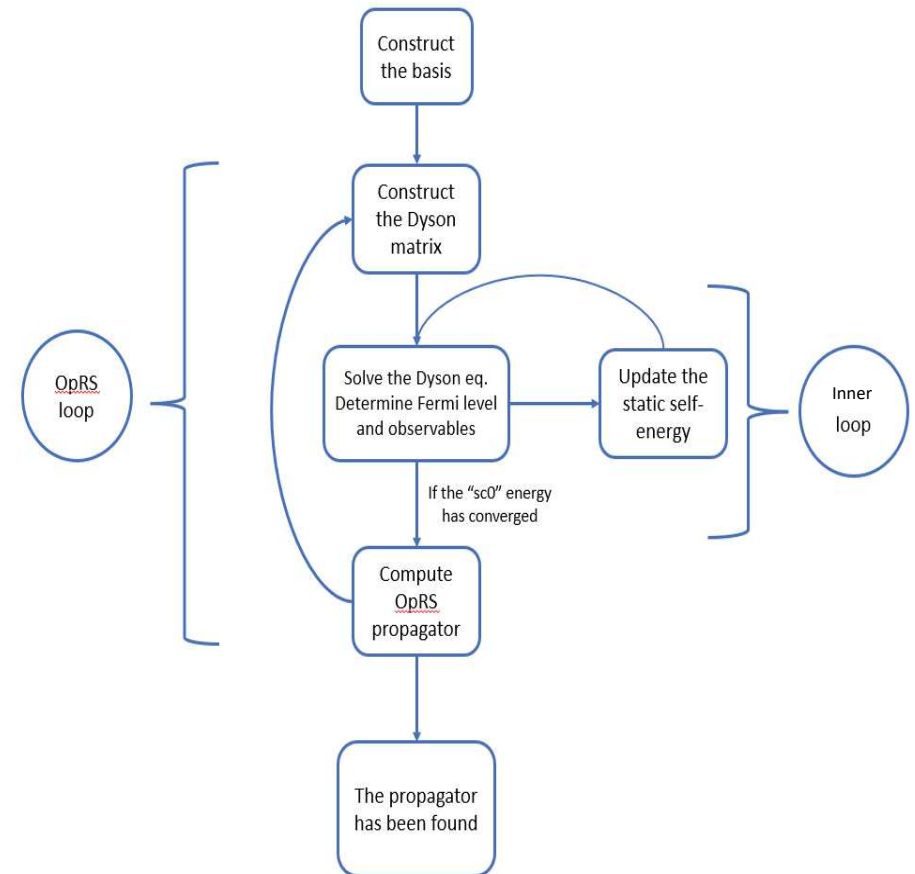
- Dyson ADC(3) needs s.p. energies: Optimized ref. states from Grkv

$$\mathcal{G}_{\alpha\beta}^{g_1 g_2}(\omega) = \mathcal{G}_{\alpha\beta}^{OpRS, g_1 g_2}(\omega) + \sum \mathcal{G}_{\alpha\gamma}^{OpRS, g_1 g_3}(\omega) \Sigma_{\gamma\delta}^*, g_3 g_4(\omega) \mathcal{G}_{\alpha\delta}^{g_4 g_2}(\omega)$$

$$\mathcal{G}_{\alpha\beta}^{g_1 g_2}(\omega) \rightarrow \mathcal{G}_{\alpha\beta}^{OpRS, g_1 g_2}(\omega), \dots, \omega^{OpRS}(k) \rightarrow \varepsilon^{OpRS}(k) = \mu \pm \omega^{OpRS}(k)$$

- Spectra function

$$S(k, \omega) = \mp \frac{1}{\pi} \Im m \mathcal{G}_{k=k'}^{g_1=g_2=1}(\omega)$$



# Combined Gkv-ADC(1) + Dys ADC(3)

- Self energy:

$$\Sigma_{\alpha\beta}^* g_1 g_2(\omega) = \underbrace{\Sigma_{\alpha\beta}^{(\infty)} g_1 g_2}_{\text{Gorkov-ADC(1)}} + M_{\alpha}^{\dagger} \left[ \frac{1}{\omega - E_{2p1h} + i\eta} \right] M_{\beta} + N_{\alpha} \left[ \frac{1}{\omega - E_{2h1p} - i\eta} \right] N_{\beta}^{\dagger}$$

Dyson-ADC(3)  
(only normal part!)

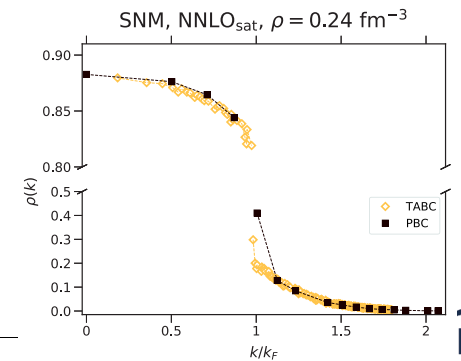
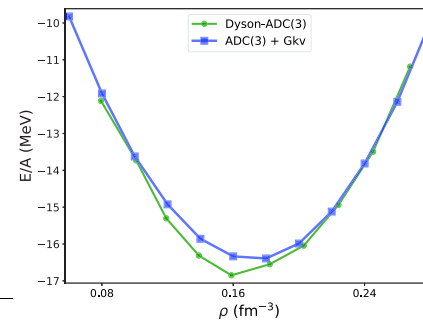
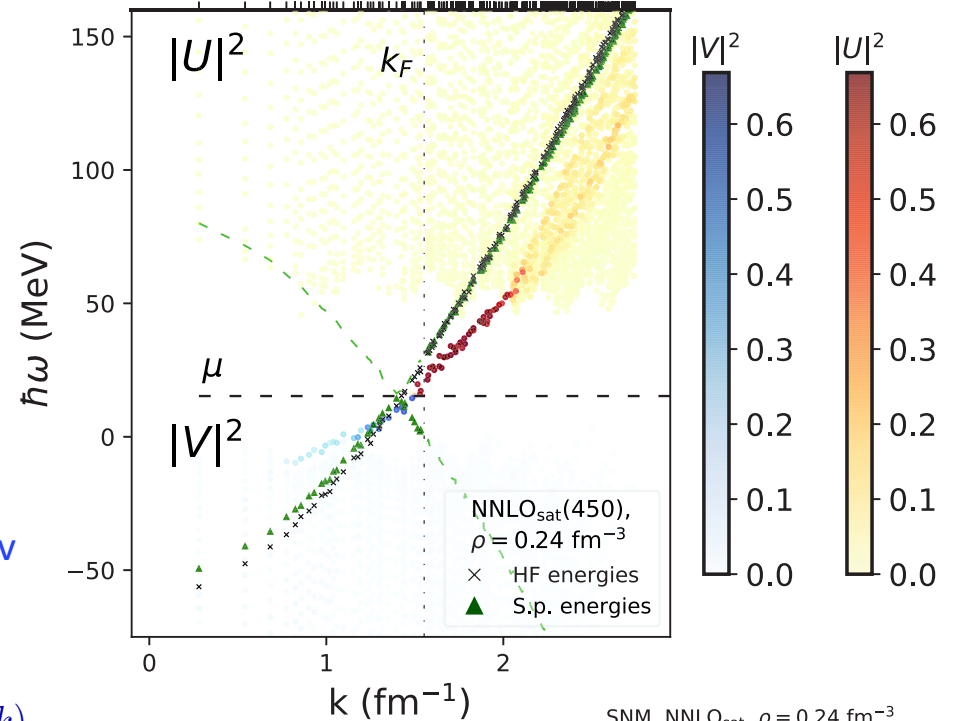
- Dyson ADC(3) needs s.p. energies: Optimized ref. states from Grkv

$$\mathcal{G}_{\alpha\beta}^{g_1 g_2}(\omega) = \mathcal{G}_{\alpha\beta}^{OpRS, g_1 g_2}(\omega) + \sum_{\gamma} \mathcal{G}_{\alpha\gamma}^{OpRS, g_1 g_3}(\omega) \Sigma_{\gamma\delta}^* g_3 g_4(\omega) \mathcal{G}_{\alpha\delta}^{g_4 g_2}(\omega)$$

$$\mathcal{G}_{\alpha\beta}^{g_1 g_2}(\omega) \rightarrow \mathcal{G}_{\alpha\beta}^{OpRS, g_1 g_2}(\omega), \quad \omega^{OpRS}(k) \rightarrow \varepsilon^{OpRS}(k) = \mu \pm \omega^{OpRS}(k)$$

- Spectra function

$$S(k, \omega) = \mp \frac{1}{\pi} \Im m \mathcal{G}_{k=k'}^{g_1=g_2=1}(\omega)$$



# Summary

Thank you for your attention!!!

- Optimised reference states stabilise computations — valid alternative to Nat. Orb., ecc...
- Improved spectroscopy from polarization propagators improve with should-phonons but current implementation are still outdated.
- Diagrammatic Monte Carlo is a promising method to go forward on high precision simulations.
- SCGF Gorkov/ADC(3) computations in nuclear matter in the way. Applications to Nuclear DFT.

And thanks to my **collaborators** (over the years...):



*G. Colò, E. Vigezzi, S. Brolli*



*P. Navrátil*



*M. Vorabbi, P. Arthuis*



*C. Giusti, P. Finelli*



*V. Somà, T. Duguet, A. Scalesi*



LUND

*A. Idini*